

The Space Oblique Conic Projection

Liucheng Ren¹, Keith C. Clarke², Chenghu Zhou³

ABSTRACT: The problem of determining a suitable map projection for side-looking synthetic aperture radar (SAR) satellite imagery is examined. Using a foundation in dynamic mathematics, a new Space Oblique Conic projection (SOC) is proposed that is specifically designed for side-looking radar imagery. The geometric model of SOC is formalized, and the ground track projection of the central line of a side-looking field of view is established based on this model. The forward and inverse formulas for the SOC projection are derived and the projection's pattern of distortion is discussed. As an example, SEASAT-A radar imagery is considered, and a particular SOC projection model for this satellite derived.

KEYWORDS: Space map projection, Space oblique conic projection, side-looking radar, projection distortion

Introduction

Side-looking radars have enjoyed continued success in mapping earth phenomena--including geology, vegetation, forestry, and topography--since the 1960s from aircraft, and from the 1970s from space platforms (Simonett, 1970; Leberl, 1976; Henderson and Lewis, 1998). While recent attention has turned to mapping terrain, which can be achieved with radar in all weathers and illumination conditions, and to high resolution methods such as interferometric SAR, nevertheless the string of successful radar satellites (SEASAT, SLAR, RADARSAT, [TerraSAR-X](#), Magellan, SIR-C, etc.) means that radar data for earth are ubiquitous, and now are available over a 50 year timespan. Work to date on mapping from SAR has been based on single images, stereo, and image overlap (Leberl, 1976). Most solutions for earth geometry for small scale mapping have used ground truth and rubber-sheeting style geometric rectifications. In this paper, we seek a purely analytic solution based on orbital and radar geometry, and on map projections, in particular the class of map projections known as *space projections* (Ren and Zhu 2001; Ren 2003).

Space map projections are dynamic map projections specifically established for a remotely sensed satellite platform, in which both geometry and time play a part in determining the structure of the image. It is desirable to specify the geometry of a map projection model so that satellite imagery can be geo-rectified to earth-based coordinate systems for cartography and further image applications. A space map projection is necessary to establish the precise processing and cartography of side-looking radar imagery, in particular from Synthetic Aperture Radars that generally image at a fixed angle to the vertical. To date, few have considered the geometry of side-looking radar,

and fewer still have considered a direct map projection of the data. A simple view of the radar imaging geometry is shown in figure 1.

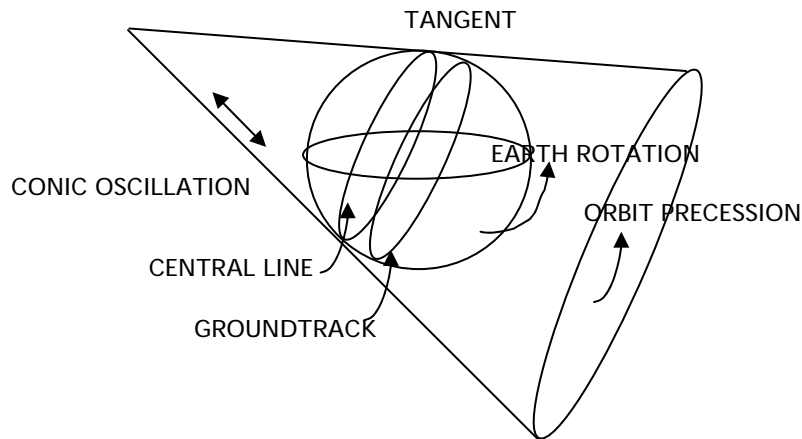


Figure.1 Geometric model of the SOC projection

The concept of space projections is generalized from the initial work of Colvocoresses, who pioneered the field while cartographic coordinator for earth satellite mapping at USGS in 1974 with the space oblique Mercator projection (SOM) (Colvocoresses, 1974). Since then, other space projections have been developed and the SOM equations derived (Junkins and Taylor, 1977; Snyder, 1977). More recently, work on space projections has been focused in China (Yang, 1996, 1999; Liucheng, 2003; Liucheng et al., 2010).

Side-looking radar (SLR) is an active microwave remote sensing system, the imagery data is obtained by sending a radar pulse toward the ground, then receiving the reflected pulse wave after its interactions with the ground surface. The mathematical foundation for the system geometry is an important problem for cartographers to solve, so that the imagery can be precisely geometrically corrected, and the errors minimized. The geometric distortion of SLR imagery can be influenced by many factors, such as the orientation, roll, pitch and yaw of the satellite, the rotation and curvature of the earth, the orbital precession of the satellite and the selection of the image projection plane, among many other factors. The selection of a suitable map projection is very important for high precision and accurate rectification of SLR imagery.

Existing mathematical models for SLR representation are based on instantaneous imaging equations which, in turn, are built point by point or row by row for the scanner's sweep across the earth's surface (Qian, et. al, 1992). However, these models cannot represent all of the image data, which is obtained continuously by the radar. The Space Oblique Mercator projection, the Conformal Space Projection (CSP) (Cheng, 1996) and other space map projections have all been designed specifically for satellite imagery that is scanned around a nadir ground track, such as SPOT and TM imagery. The precision of the projection can only satisfy the demands of cartography within $\pm 1^\circ$ of latitude and longitude around the ground track. However, the central line of the swath for SLR is about 270km away from the ground track of the satellite generally, outside the region of $\pm 1^\circ$ around the ground track of the satellite. For example, the effective imaging region of the SLR imaging system of SEASAT-A was $\pm 2^\circ$ away from the ground track of the

satellite (Leberl, 1981). Obviously, the SOM and CSP projections are not suitable for representing SLR imagery, because the precisions of the projections do not satisfy cartographic accuracy requirements. Our solution to this problem is to design a space map projection specifically for the representation of the SLR image data.

The aim of this paper is to describe the space oblique conic projection (SOC) for SLR image data based on simulating the physical processes and geometric relations of imaging with SLR. A space projection has the characteristic of establishing the corresponding relation between pixels and ground points approximately while keeping the central line of the SLR swath distortion-free. SOC is a new time-related projection designed for the precise rectification of satellite based SLR.

Geometric principles of the Space Oblique Conic Projection

While accounting for the factors of satellite geometry and movement, for the rotation of the earth and for the satellite's orbital precession, assume a cone that is defined by a circular orbit (Figure 1) with the projection surface tangent to the spheroid of the earth, and for which the tangent line is the central line of a SLR swath. There exists a set of relative movement relations among the cone, the satellite and the earth, making up four principal motions: (1) the satellite's scanner sweep across the earth's surface; (2) the satellite's orbit; (3) the earth's rotation; and (4) the earth's orbital precession. To keep these motions from distorting the SLR image, the conic surface of the projection is made to oscillate along its axis at a compensatory rate that varies with latitude. Simulating the physical process of SLR imaging according to this model, a new projection is derived as follows. In order to solve the projection model, two conditions must be assumed: 1. zero length distortion on the central line of the image swath; and 2. conformality, or local "shape" preservation.

Because the space oblique conic projection is a periodic function of time t , its formula can be denoted as

$$x = f_1(\phi, \lambda, t) \quad , \quad y = f_2(\phi, \lambda, t)$$

Ground Track of the central line for a side-look region

In order to establish the formula for the SOC, first the projection formula of the groundtrack projection of the central line of the side-look region must be established.

Denoting the central line as L . Assuming $A(\phi_L, \lambda_L, t)$ is any point on L , the corresponding projection on the projection plane is $B(x_L, y_L, t)$.

Maintaining length Suppose the arc length of the central line L at time t is:

$$s = \int_0^t v_L(\tau) d\tau \quad (3.1)$$

The corresponding arc length on the projection plane is:

$$s' = \int_0^t \sqrt{\left(\frac{dx_L}{d\tau}\right)^2 + \left(\frac{dy_L}{d\tau}\right)^2} d\tau \quad (3.2)$$

where $v_L(t)$ is the instantaneous velocity of the scanning point at time t on the central line L of the side-look region. In order to preserve length, that is $s = s'$, then

$$v_L^2 = \left(\frac{dx_L}{dt}\right)^2 + \left(\frac{dy_L}{dt}\right)^2 \quad (3.3)$$

Maintaining Curvature In order to preserve the shape of projected region, the curvature radius of the central line L must be equal to the instantaneous curvature radius of its projection $\rho(t)$ in the projection plane, that is:

$$\left(\frac{d^2 x_L}{ds^2}\right)^2 + \left(\frac{d^2 y_L}{ds^2}\right)^2 = \frac{1}{\rho^2(t)} \quad (3.4)$$

Combining formulas (3.3) and (3.4), the equations of the ground track projection can be solved as:

$$\begin{cases} \frac{dx_L}{dt} = v_L(t) \cos f \\ \frac{dy_L}{dt} = v_L(t) \sin f \\ \frac{df}{dt} = \frac{v_L(t)}{\rho(t)} \end{cases} \quad (3.5)$$

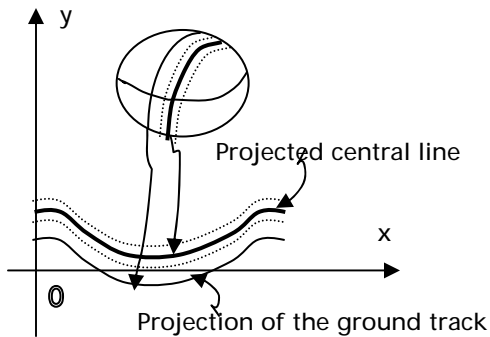


Figure 2 Projection of ground track line

Therefore, the projection of the central line L of each side-look region is

$$\left\{ \begin{array}{l} f = \int_0^t \frac{v_L(\tau)}{\rho(\tau)} d\tau \\ x_L(t) = \int_0^t v_L(\tau) \cos(f(\tau)) d\tau \\ y_L(t) = y_L(0) + \int_0^t v_L(\tau) \sin(f(\tau)) d\tau \end{array} \right. \quad (3.6)$$

Calculation of $v_L(t)$ and $\rho(t)$

Figure 3 shows the vectors of the satellite's movement. Suppose the velocity vector of the satellite is $\vec{V}(t) = \{\dot{x}, \dot{y}, \dot{z}\}$, then the secant vector which is vertical to the groundtrack circle is:

$$\vec{U} = \vec{r} \times \vec{V} = \{\dot{z}y - y\dot{z}, \dot{x}z - z\dot{x}, \dot{y}x - x\dot{y}\} \quad (3.7)$$

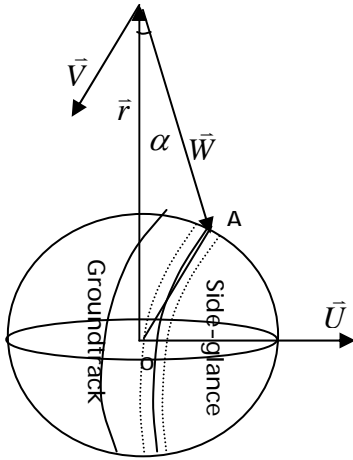


Figure 3. Satellite movement vectors

Assuming the scanning vector is $\vec{w} = \{w_1, w_2, w_3\}$ and the angle between the scanning vector \vec{w} and satellite vector \vec{r} is α , then:

$$\vec{w} = a_1 \vec{r} + a_2 \vec{U}$$

where

$$a_1 = \frac{\vec{w} \cdot \vec{r}}{|\vec{r}|^2} = \frac{|\vec{w}| \cdot |\vec{r}| \cos(\pi - \alpha)}{|\vec{r}|^2} = -\frac{|\vec{w}| \cos \alpha}{|\vec{r}|}$$

$$a_2 = \frac{\vec{w} \cdot \vec{U}}{|\vec{U}|^2} = \frac{|\vec{w}| \cdot |\vec{U}| \cos(\pi/2 - \alpha)}{|\vec{U}|^2} = \frac{|\vec{w}| \sin \alpha}{|\vec{U}|}$$

$$\begin{aligned}
 \text{then } \bar{w} &= |\bar{w}| \left[-\frac{\cos \alpha}{|\bar{r}|} \bar{r} + \frac{\sin \alpha}{|\bar{U}|} \bar{U} \right] \\
 &= |\bar{w}| \left[-\frac{\cos \alpha}{\sqrt{x^2 + y^2 + z^2}} \{x, y, z\} + \frac{\sin \alpha}{|\bar{V}||\bar{r}|} \bar{U} \right] \quad (3.8)
 \end{aligned}$$

where

$$|\bar{w}| = |\bar{r}| \cos \alpha - \sqrt{R^2 - |\bar{r}|^2 \sin^2 \alpha} \quad , \quad (3.9)$$

The condition $\sin \alpha \leq R/|\bar{r}|$ is required, so:

$$w_1 = |\bar{w}| \left[-\frac{x \cos \alpha}{|\bar{r}|} - \frac{\sin \alpha}{|\bar{V}||\bar{r}|} (\dot{y}z - y\dot{z}) \right] \quad (3.10)$$

$$w_2 = |\bar{w}| \left[-\frac{y \cos \alpha}{|\bar{r}|} - \frac{\sin \alpha}{|\bar{V}||\bar{r}|} (\dot{z}x - \dot{x}z) \right] \quad (3.11)$$

$$w_3 = |\bar{w}| \left[-\frac{z \cos \alpha}{|\bar{r}|} - \frac{\sin \alpha}{|\bar{V}||\bar{r}|} (\dot{x}y - \dot{y}x) \right] \quad (3.12)$$

$$\frac{d}{dt} |\bar{w}| = \frac{\cos \alpha (x\dot{x} + y\dot{y} + z\dot{z})}{|\bar{r}|} + \frac{\sin^2 \alpha (x\dot{x} + y\dot{y} + z\dot{z})}{\sqrt{R^2 - |\bar{r}|^2 \sin^2 \alpha}} \quad (3.13)$$

According to the formulas above, the vector \bar{R}_L can be defined as:

$$\bar{R}_L = \bar{r} + \bar{w} = (x + w_1)\bar{i} + (y + w_2)\bar{j} + (z + w_3)\bar{k} \quad (3.14)$$

$$\dot{\bar{R}}_L = \dot{\bar{r}} + \dot{\bar{w}} = (\dot{x} + \dot{w}_1)\bar{i} + (\dot{y} + \dot{w}_2)\bar{j} + (\dot{z} + \dot{w}_3)\bar{k} \quad (3.15)$$

$$\ddot{\bar{R}}_L = \ddot{\bar{r}} + \ddot{\bar{w}} = (\ddot{x} + \ddot{w}_1)\bar{i} + (\ddot{y} + \ddot{w}_2)\bar{j} + (\ddot{z} + \ddot{w}_3)\bar{k} \quad (3.16)$$

According to equations 3.7 through 3.12, we have:

$$v_L^2(t) = \dot{w}_1^2 + \dot{w}_2^2 + \dot{w}_3^2$$

$$\begin{aligned}
 &= \left(\frac{d}{dt} |\bar{w}| \right)^2 + |\bar{w}|^2 \sin^2 \alpha \left(\frac{d}{dt} \left(\frac{|\bar{U}|}{|\bar{V}| |\bar{r}|} \right) \right)^2 + \frac{|\bar{V}|^2 \cos^2 \alpha}{|\bar{r}|^2} |\bar{w}|^2 \\
 &- |\bar{w}|^2 \left(\frac{\sin 2\alpha}{|\bar{V}| |\bar{r}|^2} (\ddot{x}(\dot{y}z - \dot{z}y) + \ddot{y}(\dot{z}x - \dot{x}z) + \ddot{z}(\dot{x}y - \dot{y}x)) \right) \quad (3.17)
 \end{aligned}$$

Denoting $\bar{T}_L(t) = \bar{R}_L = \{\dot{x} + \dot{w}_1, \dot{y} + \dot{w}_2, \dot{z} + \dot{w}_3\}$, then the secant vector which is vertical to the central line of the side-looking region at the time instant t is

$$\begin{aligned}
 \bar{U}_L(t) = \bar{R}_L \times \bar{T}_L = & \{(y + w_2)(\dot{z} + \dot{w}_3) - (\dot{y} + \dot{w}_2)(z + w_3), (\dot{x} + \dot{w}_1)(z + w_3) - (x + w_1)(\dot{z} + \dot{w}_3), \\
 & (\dot{y} + \dot{w}_2)(x + w_1) - (y + w_2)(\dot{x} + \dot{w}_1)\} \quad (3.18)
 \end{aligned}$$

$$\frac{1}{\rho(t)} = \bar{U}_L \cdot \frac{d^2}{ds^2} \bar{R}_L = \bar{U}_L \cdot \left(\frac{1}{v_L^2} \ddot{\bar{R}}_L - \frac{\dot{v}_L}{v_L^3} \dot{\bar{R}}_L \right) = \frac{1}{v_L^2} (\bar{U}_L \cdot \ddot{\bar{R}}_L) - \frac{\dot{v}_L}{v_L^3} (\bar{U}_L \cdot \dot{\bar{R}}_L) = \frac{1}{v_L^2} (\bar{U}_L \cdot \ddot{\bar{R}}_L) \quad (3.19)$$

then

$$\begin{aligned}
 \frac{1}{\rho(t)} = \frac{1}{v_L^2} & \{(\ddot{x} + \ddot{w}_1)[(\dot{z} + \dot{w}_3)(y + w_2) - (\dot{y} + \dot{w}_2)(z + w_1)] \\
 & + (\ddot{y} + \ddot{w}_2)[(\dot{x} + \dot{w}_1)(z + w_3) - (\dot{z} + \dot{w}_3)(x + w_2)] \\
 & + (\ddot{z} + \ddot{w}_3)[(x + w_1)(\dot{y} + \dot{w}_2) - (\dot{x} + \dot{w}_1)(y + w_2)]\} \quad (3.20)
 \end{aligned}$$

Calculation of the integrals $\int_0^t v_L(\tau) \cos f d\tau$, $\int_0^t v_L(\tau) \sin f d\tau$ **and** $\int_0^t \frac{v_L(\tau)}{\rho(\tau)} d\tau$

According to formula 3.7, we know that:

$$\dot{x}_L = v_L(t) \cos f \quad , \quad \dot{y}_L = v_L(t) \sin f \quad , \quad \dot{f} = \frac{v_L(t)}{\rho(t)}$$

Given the appropriate formulas for the calculation of $v_L(t)$ and $\rho(t)$ above, and the given initial conditions $\{x_L(0), y_L(0), f(0)\}$, then the differential equations above can be integrated numerically. However, it is computationally expensive to carry out these integrations many times, and since these integrals have been found to be very smooth functions of time, they can be conveniently and accurately replaced by their harmonic series as:

$$x_L(t) = a_{x0}t + \sum_{n=0}^{+\infty} \left\{ a_{xn} \sin \frac{n\pi t}{P_2} + b_{xn} \cos \frac{n\pi t}{P_2} \right\} \equiv \int_0^t v_L(\tau) \cos f d\tau \quad (3.21a)$$

$$y_L(t) = a_{y0}t + \sum_{n=0}^{+\infty} \left\{ a_{yn} \sin \frac{n\pi t}{P_2} + b_{yn} \cos \frac{n\pi t}{P_2} \right\} \equiv \int_0^t v_L(\tau) \sin f d\tau \quad (3.21b)$$

$$f(t) = a_{f0}t + \sum_{n=0}^{+\infty} \left\{ a_{fn} \sin \frac{n\pi t}{P_2} + b_{fn} \cos \frac{n\pi t}{P_2} \right\} \equiv \int_0^t \frac{v_L}{\rho} d\tau \quad (3.21c)$$

where P_2 is the orbital period,

$$a_{x0} = \frac{1}{P_2} \int_0^{P_2} v_L(t) \cos f(t) dt, \quad (3.22a)$$

$$a_{y0} = \frac{1}{P_2} \int_0^{P_2} v_L(t) \sin f(t) dt, \quad (3.22b)$$

$$a_{f0} = \frac{1}{P_2} \int_0^{P_2} \frac{v_L(t)}{\rho(t)} dt \quad (3.22c)$$

$$a_{xn} = \frac{2}{P_2} \int_0^{P_2} [x_L(t) - a_{x0}t] \sin \frac{n\pi t}{P_2} dt, \quad (3.23a)$$

$$b_{xn} = \frac{2}{P_2} \int_0^{P_2} [x_L(t) - a_{x0}t] \cos \frac{n\pi t}{P_2} dt \quad (3.23b)$$

$$a_{yn} = \frac{2}{P_2} \int_0^{P_2} [y_L(t) - a_{y0}t] \sin \frac{n\pi t}{P_2} dt, \quad (3.23c)$$

$$b_{yn} = \frac{2}{P_2} \int_0^{P_2} [y_L(t) - a_{y0}t] \cos \frac{n\pi t}{P_2} dt \quad (3.23d)$$

$$a_{fn} = \frac{2}{P_2} \int_0^{P_2} [f(t) - a_{f0}t] \sin \frac{n\pi t}{P_2} dt, \quad (3.23e)$$

$$b_{fn} = \frac{2}{P_2} \int_0^{P_2} [f(t) - a_{f0}t] \cos \frac{n\pi t}{P_2} dt \quad (3.23f)$$

Using the Runge-Kutta algorithm (Butcher, 2003) and the calculations leading to instantaneous $v_L(t)$ and $\rho(t)$, all the coefficients above can be determined. A computational example is given later in the paper.

The Space Oblique Conic Projection Formula

In this section, we present the derivation of the map projection approximately in the manner it was developed and the formula will be deduced based on the projection formula of the central line of side-glance region already presented. Since the satellite orbit is oblique to the equator generally, the transformation at the equator is needed in order to use the static conformal conic projection formula expediently.

4.1 Transformation at the Equator

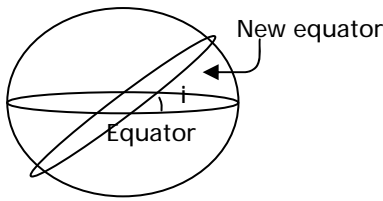


Figure 4 Transformed equator

Let the ground track of a SLR satellite be the new equator, then the obliquity between the equator and the satellite orbit is i (Figure 4). According to Snyder (1977) and Yang (1989), if the coordinates (ϕ, λ) of a latitude and longitude position are known, then the coordinates (ϕ', λ') of new latitude and longitude are:

$$\left. \begin{aligned} tg\lambda' &= tg\lambda_t \cos i + tg\phi \sin i / \cos \lambda_t \\ \sin \phi' &= \sin \phi \cos i - \cos \phi \sin \lambda_t \sin i \\ \lambda_t &= \lambda + (P_2/P_1)\lambda' \end{aligned} \right\} (4.1)$$

The new latitude and longitude can be solved using iteration. Conversely, if the transformed latitude and longitude (ϕ', λ') are known, then the original latitude and longitude (ϕ, λ) can be solved by:

$$\left. \begin{aligned} \sin \phi &= \cos i \sin \phi' + \sin i \cos \phi' \sin \lambda' \\ tg\lambda_t &= tg\lambda' \cos i - \sin i tg\phi' / \cos \lambda' \\ \lambda &= \lambda_t - (P_2/P_1)\lambda' \end{aligned} \right\} (4.2)$$

Detailed formulation of the space oblique conic projection

With reference to figure 5, we consider the projection of all sensed points within a finite region on the reference ellipsoid, centered on the ground track onto the map plane. This problem is approached using the simple notion that very small displacements are

made on the ellipsoid from a locally very-nearly straight line. Accordingly, displacements near the ground track from nearby points might be well-approximated by displacements near the equator of an oblique conic projection (where the oblique equator is locally tangent to the ground track). The resulting map projection (based on this approximation) is developed such that conformality and length preservation are rigorous satisfied only along the ground track, but the approximation remains accurate within several hundred kilometers of the satellite ground track.

Assuming zero Doppler effect, when the satellite flies at instant t , the geometric relation of the conformal conic projection that is tangent to the central line of the side-looking region is shown as in figure 6, and the angle between the direction of satellite flight and the x axis is:

$$\varepsilon = \arctg\left(\frac{\dot{y}_L}{\dot{x}_L}\right) \quad (4.3)$$

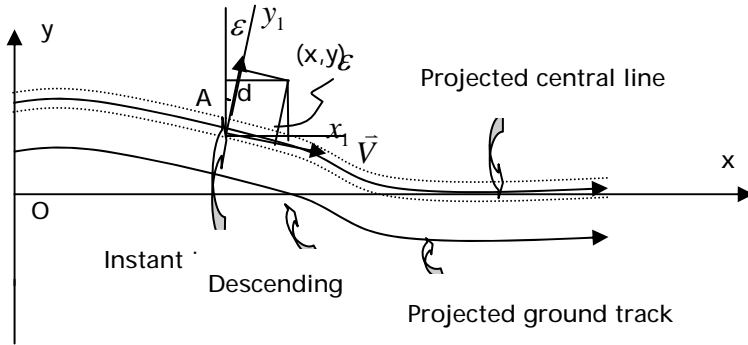


Figure 5 Geometry of the space oblique conic projection

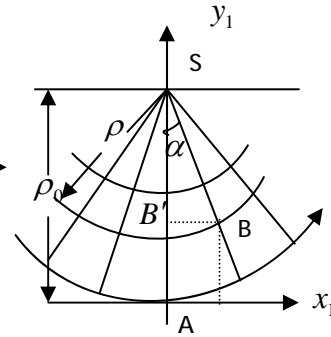


Figure 6 Conformal conic projection

In figure 5, rotating the instantaneous Cartesian geometry x_1Ay_1 to an angle ε , we have:

$$\begin{cases} x_2 = x_1 \cos \varepsilon - y_1 \sin \varepsilon \\ y_2 = x_1 \sin \varepsilon + y_1 \cos \varepsilon \end{cases} \quad (4.4)$$

According to Wu, et.al. (1989), taking any point A on the ground track as the origin point and the direction of a satellite track as the x_1 axis we can create a dynamic Cartesian system, as shown in figure 6. Suppose $B(\phi', \lambda')$ is arbitrary point in the side-look region, then the conformal conic projection corresponding to the new equator is:

$$\rho = f(\phi') = \frac{C}{U^\alpha}, \quad \delta = \alpha \lambda' \quad (4.5)$$

$$x_1 = \rho \sin \delta, \quad y_1 = \rho_0 - \rho \cos \delta \quad (4.6)$$

where: $\rho_0 = R \operatorname{ctg} \phi'_0$, $C = R \operatorname{ctg} \phi'_0 U_0^\alpha$, $\alpha = \sin \phi'_0$, $U = \operatorname{tg} \left(\frac{\pi}{4} + \frac{\phi'}{2} \right)$, $\phi'_0 = \frac{s_0}{R}$

R is the earth's radius, s_0 is the distance from the central line side-look region to the ground track.

Folding the coordinate system x_2Ay_2 with xoy together, for any point B in the side-look region, its projection coordinates in the xoy system are:

$$x = \int_0^t v_L \cos f d\tau + d \cos(\delta + \varepsilon) + d_0 \sin \varepsilon \quad (4.7)$$

$$y = \int_0^t v_L \sin f d\tau + y_0(0) - d \sin(\varepsilon + \delta) + d_0 \cos \varepsilon \quad (4.8)$$

where

t = the orbital time since the start ;

$v_L(t)$ = the instantaneous velocity of the point A on the central line of the side-look region corresponding to the earth at the time instant t ;

$\rho(t)$ = the instantaneous curvature radius at point A on the central line;

$$f \equiv \int_0^t \frac{v_L(\tau)}{\rho(\tau)} d\tau ; \quad (4.9)$$

$$d = \frac{C}{U^\alpha} ; C = R \operatorname{ctg} \phi'_0 U_0^\alpha ; d_0 = R \operatorname{ctg} \phi'_0 ; \quad (4.10)$$

$$U = \operatorname{tg} \left(\frac{\pi}{4} + \frac{\phi'}{2} \right) ; U_0 = \operatorname{tg} \left(\frac{\pi}{4} + \frac{\phi'_0}{2} \right) ; \quad (4.11)$$

$\alpha = \sin \phi'_0$; $\phi'_0 = \frac{s_0}{R}$ (s_0 is the distance from A to the groundtrack at time t) ;

$$\delta = \alpha \lambda' ; \quad (4.12)$$

Latitude $\phi^{(t)}$ and longitude $\lambda^{(t)}$ of side-looking point B at time t

Assuming a side-look point is $B(\phi, \lambda)$ along the satellite orbit at the instant t --that is the beam points to $B(\phi, \lambda)$ --then the geographic coordinate of the corresponding point B_0 on

the central line of side-look region is $(\phi_0(t), \lambda_0(t))$. With reference to figure 7, assuming zero Doppler effect, $B(\phi, \lambda)$ and $B_0(\phi_0, \lambda_0)$ are located in the plane which is determined by the unit normal vector \bar{n} and the pulse vector \bar{w} , that is, the identity equation is satisfied:

$$F(t) \equiv [(\bar{w} \times \bar{n}) \cdot \Delta \bar{R}](t) = 0 \quad (5.1)$$

where

$$\Delta \bar{R} = \bar{R} - \bar{R}_0 = (R_x - R_{x0})\bar{i} + (R_y - R_{y0})\bar{j} + (R_z - R_{z0})\bar{k}$$

(the vector from $B_0(\phi_0, \lambda_0)$ to $B(\phi, \lambda)$),

$$R_x = R \cos \phi \cos \lambda, \quad R_{x0} = R \cos \phi_0 \cos \lambda_0,$$

$$R_y = R \cos \phi \sin \lambda, \quad R_{y0} = R \cos \phi_0 \sin \lambda_0,$$

$$R_z = R \sin \phi, \quad R_{z0} = R \sin \phi_0;$$

$$\bar{w} = w_x \bar{i} + w_y \bar{j} + w_z \bar{k} = \bar{R} - \bar{r},$$

$$w_x = R_x - x = R \cos \phi \cos \lambda - x,$$

$$w_y = R_y - y = R \cos \phi \sin \lambda - y, \quad w_z = R_z - z = R \sin \phi - z;$$

$$\bar{n} = \cos \phi \cos \lambda \bar{i} + \cos \phi \sin \lambda \bar{j} + \sin \phi \bar{k};$$

Substituting the vectors above into equation 5.1, we have

$$\begin{aligned} & (z \cos \phi \sin \lambda - y \sin \phi)(\cos \phi \cos \lambda - \cos \phi_0 \cos \lambda_0) \\ & + (x \sin \phi - z \cos \phi \cos \lambda)(\cos \phi \sin \lambda - \cos \phi_0 \sin \lambda_0) \\ & + (y \cos \phi \cos \lambda - x \cos \phi \sin \lambda)(\sin \phi - \sin \phi_0) = 0 \end{aligned} \quad (5.2)$$

Similarly, formula 5.2 is also true for the transformation of geographic coordinates ϕ', λ' and ϕ'_0, λ'_0 .

According to Snyder (1977) and assuming zero Doppler effect, $\lambda' = \lambda'_0 = 2\pi/P_2$, $\phi'_0 = s_0/R$ are known. Substituting λ', λ'_0 and ϕ'_0 into equation 5.2, the relation of ϕ' at

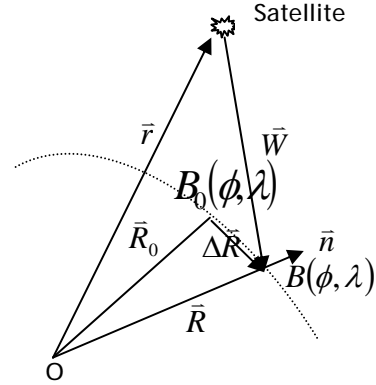


Figure 7 Displacement of the satellite side-look point

time t can be solved. Then substituting ϕ'_0, λ'_0 and ϕ', λ' into equation 4.1 respectively, ϕ_0, λ_0 and ϕ, λ can be computed using iterative methods.

Inverse transformation

Selecting the initial latitude and longitude $\phi^{(0)} = \phi_L(t), \lambda^{(0)} = \lambda_L(t)$ for any time t , and substituting $\phi^{(0)}$ and $\lambda^{(0)}$ into equations 4.7 and 4.8, then the corresponding coordinates $x^{(0)}, y^{(0)}$ in the SOC can be obtained. Constructing the iterative formula:

$$\begin{Bmatrix} \phi^{(k+1)} \\ \lambda^{(k+1)} \end{Bmatrix} = \begin{Bmatrix} \phi^{(k)} \\ \lambda^{(k)} \end{Bmatrix} + \begin{bmatrix} \left. \frac{\partial x}{\partial \phi} \right|^{(k)} & \left. \frac{\partial x}{\partial \lambda} \right|^{(k)} \\ \left. \frac{\partial y}{\partial \phi} \right|^{(k)} & \left. \frac{\partial y}{\partial \lambda} \right|^{(k)} \end{bmatrix}^{-1} \begin{Bmatrix} x - x^{(k)} \\ y - y^{(k)} \end{Bmatrix} \quad (6.1)$$

The matrix of partial derivatives can also be obtained from equations 4.7 and 4.8. The coordinates $x^{(k)}, y^{(k)}$ of SOC for the k^{th} step can be obtained by substituting $\phi^{(k)}, \lambda^{(k)}$ into equations 4.7 and 4.8. $\phi(t), \lambda(t)$ can be obtained with a relatively small numbers of iterations, 4 or 5 steps generally, according to equation 6.1.

Projection distortion analysis

Taking partial derivatives of equations 4.7 and 4.8 yields:

$$\frac{\partial x}{\partial \phi} = \frac{\partial x_L}{\partial \phi} + \frac{\partial d}{\partial \phi} \cos(\delta + \varepsilon) - d \sin(\delta + \varepsilon) \left(\frac{\partial \delta}{\partial \phi} + \frac{\partial \varepsilon}{\partial \phi} \right) + d_0 \cos \varepsilon \frac{\partial \varepsilon}{\partial \phi}$$

$$\frac{\partial y}{\partial \phi} = \frac{\partial y_L}{\partial \phi} - \frac{\partial d}{\partial \phi} \sin(\delta + \varepsilon) - d \cos(\delta + \varepsilon) \left(\frac{\partial \delta}{\partial \phi} + \frac{\partial \varepsilon}{\partial \phi} \right) - d_0 \sin \varepsilon \frac{\partial \varepsilon}{\partial \phi}$$

To compact the notation, we make use of the symbol " $\phi \rightarrow \lambda, t$ " whenever the identical equation for λ or t results by simply replacing ϕ by λ or t .

(1) Calculation of each partial derivative of x_L and y_L

$$\text{Because } x_L \text{ and } y_L \text{ are functions of time } t, \quad \frac{\partial x_L}{\partial \phi} = \frac{\partial x_L}{\partial \lambda} = \frac{\partial y_L}{\partial \phi} = \frac{\partial y_L}{\partial \lambda} = 0$$

$$\frac{\partial x_L}{\partial t} = v_L(t) \cos[f(t)], \quad \frac{\partial y_L}{\partial t} = v_L(t) \sin[f(t)]$$

(2) d partials

From equations 4.10 and 4.11: $\frac{\partial d}{\partial \phi} = -\frac{\alpha C}{2U^{\alpha+1}} \sec^2\left(\frac{\pi}{4} + \frac{\phi'}{2}\right) \frac{\partial \phi'}{\partial \phi}$, $\phi \rightarrow \lambda, t$

(3) δ and ε partials

From equations 4.3 and 4.12: $\frac{\partial \delta}{\partial \phi} = \alpha \frac{\partial \lambda'}{\partial \phi}$, $\frac{\partial \varepsilon}{\partial \phi} = \frac{\dot{x}^2}{\dot{x}^2 + \dot{y}^2} \frac{\partial}{\partial \phi} \left(\frac{\dot{y}}{\dot{x}} \right)$, $\phi \rightarrow \lambda, t$

(4) ϕ', λ' partials

From equation 4.1:

$$\frac{\partial \lambda'}{\partial \phi} = \frac{P_1 \sec^2 \phi \sin i \sec \lambda_i}{P_1 \sec^2 \lambda' - P_2 \sec^2 \lambda_i \cos i - P_2 \operatorname{tg} \phi \sin i \operatorname{tg} \lambda_i \sec \lambda_i}$$

$$\frac{\partial \lambda'}{\partial \lambda} = \frac{P_1 \sec^2 \lambda_i \cos i + P_1 \operatorname{tg} \phi \sin i \operatorname{tg} \lambda_i \sec \lambda_i}{P_1 \sec^2 \lambda' - P_2 \sec^2 \lambda_i \cos i - P_2 \operatorname{tg} \phi \sin i \operatorname{tg} \lambda_i \sec \lambda_i}$$

$$\frac{\partial \phi'}{\partial \phi} = \sec \phi' \left(\cos \phi \cos i + \sin \phi \sin \lambda_i \sin i - \cos \phi \cos \lambda_i \sin i \frac{P_2}{P_1} \frac{\partial \lambda'}{\partial \phi} \right)$$

$$\frac{\partial \phi'}{\partial \lambda} = -\sec \phi' \cos \phi \cos \lambda_i \sin i \left(1 + \frac{P_2}{P_1} \frac{\partial \lambda'}{\partial \lambda} \right)$$

(5) ϕ, λ partials for t

From equations 4.1 and 5.2:

$$\frac{d\phi}{dt} = \frac{(2\pi/P_2) \sec^2 \lambda' \cos \phi \sin i \cos^3 \lambda_i + (d\phi'/dt) \cos \phi' (1 + \operatorname{tg} \phi \sin i \sin \lambda_i)}{(\cos \phi \cos i + \sin \phi \sin i \sin \lambda_i)(1 + \operatorname{tg} \phi \sin i \sin \lambda_i) + \sec \phi \sin^2 i \cos^2 \lambda_i}$$

$$\frac{d\lambda}{dt} = \frac{(2\pi/P_2) \sec^2 \lambda' (\cos \phi \cos i + \sin \phi \sin i \sin \lambda_i) \cos^2 \lambda_i + \sec^2 \phi \sin i \cos \phi' \cos \lambda_i (d\phi'/dt)}{-(\cos \phi \cos i + \sin \phi \sin i \sin \lambda_i)(1 + \operatorname{tg} \phi \sin i \sin \lambda_i) - \sec \phi \sin^2 i \cos^2 \lambda_i}$$

The projection formula

Ratio of meridian

$$m^2 = \frac{E_1(d\phi)^2 + E_3(dt)^2 + 2F_2(d\phi dt)}{M^2(d\phi)^2} = \frac{E_1 + E_3(dt/d\phi)^2 + 2F_2(dt/d\phi)}{M^2}$$

Ratio of latitude

$$n^2 = \frac{E_2(d\lambda)^2 + E_3(dt)^2 + 2F_3(d\lambda dt)}{r^2(d\lambda)^2} = \frac{E_2 + E_3(dt/d\lambda)^2 + 2F_3(dt/d\lambda)}{r^2}$$

where

$$\left. \begin{aligned} E_1 &= \left(\frac{\partial x}{\partial \phi}\right)^2 + \left(\frac{\partial y}{\partial \phi}\right)^2, E_2 = \left(\frac{\partial x}{\partial \lambda}\right)^2 + \left(\frac{\partial y}{\partial \lambda}\right)^2, \\ E_3 &= \left(\frac{\partial x}{\partial t}\right)^2 + \left(\frac{\partial y}{\partial t}\right)^2, F_1 = \frac{\partial x}{\partial \phi} \frac{\partial x}{\partial \lambda} + \frac{\partial y}{\partial \phi} \frac{\partial y}{\partial \lambda}, \\ F_2 &= \frac{\partial x}{\partial \phi} \frac{\partial x}{\partial t} + \frac{\partial y}{\partial \phi} \frac{\partial y}{\partial t}, F_3 = \frac{\partial x}{\partial \lambda} \frac{\partial x}{\partial t} + \frac{\partial y}{\partial \lambda} \frac{\partial y}{\partial t}. \end{aligned} \right\}$$

Angular distortion

The tangent of the angle between latitude and longitude is:

$$\begin{aligned} \operatorname{tg} \theta &= \operatorname{tg}(\gamma - \gamma') = \frac{\operatorname{tg} \gamma - \operatorname{tg} \gamma'}{1 + \operatorname{tg} \gamma \operatorname{tg} \gamma'} \\ &= \frac{H_1(d\phi/dt)(d\lambda/dt) + H_2(d\phi/dt) + H_3(d\lambda/dt)}{F_1(d\phi/dt)(d\lambda/dt) + F_2(d\phi/dt) + F_3(d\lambda/dt) + E_3} \\ &= \frac{H_1 + H_2(dt/d\lambda) + H_3(dt/d\phi)}{F_1 + F_2(dt/d\lambda) + F_3(dt/d\phi) + E_3(dt/d\phi)(dt/d\lambda)} \end{aligned}$$

where

$$H_1 = \frac{\partial x}{\partial \lambda} \frac{\partial y}{\partial \phi} - \frac{\partial x}{\partial \phi} \frac{\partial y}{\partial \lambda}, H_2 = \frac{\partial x}{\partial t} \frac{\partial y}{\partial \phi} - \frac{\partial x}{\partial \phi} \frac{\partial y}{\partial t}, H_3 = \frac{\partial x}{\partial \lambda} \frac{\partial y}{\partial t} - \frac{\partial x}{\partial t} \frac{\partial y}{\partial \lambda}.$$

The distortion of azimuth angle after projection is:

$$\operatorname{ctg} \alpha' = \frac{S}{H_1 M \operatorname{tg} \alpha + H_3 M^2 \operatorname{tg}^2 \alpha (dt/d\lambda)}$$

where

$$S = E_1 r^2 + F_1 M \operatorname{tg} \alpha + 2F_2 M \operatorname{tg} \alpha (dt/d\lambda) + F_3 M^2 \operatorname{tg}^2 \alpha (dt/d\lambda) + E_3 M^2 \operatorname{tg}^2 \alpha (dt/d\lambda)^2$$

Example Application

In order to get a space oblique conic projection, we take the imaging system of SEASAT as an example. SEASAT was launched on 27 June 1978 into a nearly circular 800 km orbit with an inclination of 108° , and operated for 105 days until 10 October 1978. The coordinates of SOC and its inverse can be calculated by SAR simulating data. With reference to Leberl (1981), the relevant parameters of SEASAT are: satellite orbital period $P_2 = 100$ minutes; satellite orbit is a circle; obliquity angle of the orbital plane $i = 108^\circ$; $\omega = 0.0$; $\Omega = 0.0$; orbital height $H = 800$ km; The bandwidth of side-

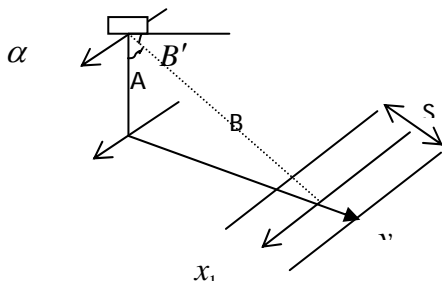


Figure 8: Geometry of the side-look strip

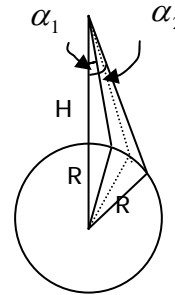


Figure 9 Angle of view

looking strip $D = 100$ km (Figure 8); view angles $\alpha_1 = 16.9^\circ$ to $\alpha_2 = 23.1^\circ$ (figure 9); and distance from the central line to the groundtrack $s_0 = 292$ km . Suppose the initial moment of satellite movement is at the descending node, selecting $t_0 = \tau = 0$, $\theta_0 = 0$; Using an earth radius of $R = 6378160.0$ m .

According to the data noted above, the pitch angle can be solved as $\alpha = s_0/H = 20.9^\circ$, the average angular velocity of satellite $\bar{n} = 2\pi/P_2 = 3.6^\circ = 0.062832$ radian/min, the transformation latitude of the central line of side-look region $\phi'_0 = s_0/R = 2.623^\circ$, the eccentric anomaly $E = \bar{n}t$ at the instant t , the rotation angle of the earth $\theta = \omega_e t$.

Regarding of the rotation of the earth, the coordinates of satellite can be obtained according to equations 3.9 through 3.14:

$$\begin{Bmatrix} x \\ y \\ z \end{Bmatrix} = (H + R) \begin{Bmatrix} \cos \omega_e t \cos \bar{n}t + \sin \omega_e t \sin \bar{n}t \cos i \\ -\sin \omega_e t \cos \bar{n}t + \cos \omega_e t \sin \bar{n}t \cos i \\ \sin \bar{n}t \sin i \end{Bmatrix} \quad (8.1)$$

According to equations 3.17 through 3.30, we have:

$$\begin{aligned}
 |\bar{V}|^2 &= (H + R)^2 [(\bar{n} - \omega_e \cos i)^2 + \omega_e^2 \cos^2 \bar{n} t \sin^2 i] \\
 |\bar{U}|^2 &= (H + R)^4 \{ \sin^2 i [\omega_e^2 \sin^2 \bar{n} t \cos^2 \bar{n} t + (\omega_e \sin^2 \bar{n} t \cos i - \bar{n})^2] \\
 &\quad + [\cos^2 (\bar{n} \cos i - \omega) + \sin^2 \bar{n} t (\omega_e \cos i - \bar{n})]^2 \} \\
 v_L^2(t) &= \left(\cos \alpha - \sqrt{\left(\frac{R}{H + R} \right)^2 - \sin^2 \alpha} \right) \cdot \{ \cos^2 \alpha |\bar{V}|^2 \\
 &\quad + \sin^2 \alpha \left(\frac{d}{dt} \left(\frac{|\bar{U}|}{|\bar{V}|} \right) \right)^2 - \frac{\sin 2\alpha}{|\bar{V}|} (\ddot{\bar{r}} \cdot \bar{U}) \} \quad (8.2)
 \end{aligned}$$

$$\begin{aligned}
 \frac{v_L(t)}{\rho(t)} &= \frac{1}{v_L} \{ (\ddot{x} + \ddot{w}_1)[(\dot{z} + \dot{w}_3)(y + w_2) - (\dot{y} + \dot{w}_2)(z + w_1)] \\
 &\quad + (\ddot{y} + \ddot{w}_2)[(\dot{x} + \dot{w}_1)(z + w_3) - (\dot{z} + \dot{w}_3)(x + w_2)] \\
 &\quad + (\ddot{z} + \ddot{w}_3)[(x + w_1)(\dot{y} + \dot{w}_2) - (\dot{x} + \dot{w}_1)(y + w_2)] \} \quad (8.3)
 \end{aligned}$$

According to equations 3.21 through 3.23:

$$\begin{aligned}
 x_L(t) &= \int_0^t v_L \cos f d\tau = 9.780451t + 0.321174 \sin \frac{\pi}{P_2} - 3.442136 \sin \frac{2\pi}{P_2} \\
 &\quad - 0.006059 \sin \frac{4\pi}{P_2} + 0.000648 \sin \frac{6\pi}{P_2} + 0.000002 \sin \frac{8\pi}{P_2} + \dots \\
 y_L(t) &= \int_0^t v_L \sin f d\tau = y_0 - 485.263782 \cos \frac{\pi}{P_2} + 4.350619 \cos \frac{3\pi}{P_2} \\
 &\quad + 0.001143 \cos \frac{5\pi}{P_2} - 0.000022 \cos \frac{7\pi}{P_2} + \dots
 \end{aligned}$$

Substituting the result above into equations 4.6 and 4.7:

$$x = 9.780451t + 3.211746 \sin \frac{\pi t}{P_2} - 0.034421 \sin \frac{2\pi t}{P_2}$$

$$\begin{aligned}
 & -0.006059 \sin \frac{4\pi t}{P_2} + 0.000648 \sin \frac{6\pi t}{P_2} + 0.000002 \sin \frac{8\pi t}{P_2} \\
 & + d \cos(\delta + \varepsilon) + d_0 \sin \varepsilon \quad (8.4)
 \end{aligned}$$

$$\begin{aligned}
 y = y_0 - 485.263782 \cos \frac{\pi t}{P_2} + 4.350619 \cos \frac{3\pi t}{P_2} \\
 + 0.001143 \cos \frac{5\pi t}{P_2} - 0.000022 \cos \frac{7\pi t}{P_2} - d \sin(\varepsilon + \delta) + d_0 \cos \varepsilon \quad (8.5)
 \end{aligned}$$

where the expressions of $\varepsilon, d, d_0, \delta$ are equations 4.6 and 4.9-4.11.

9. Conclusion

In order to satisfy the demands of cartography from side-looking radar imagery, the space map projection problem of side-looking radar image has been examined in this paper. The space oblique conic projection has been specifically designed for this kind of imagery. The geometric model and the imaging process have been simulated, by conceiving that there is a cone that is tangent to the central line of the side-look region instantaneously. According to the space geometric relations of the satellite orbit, earth rotation and the space oblique conic, the sub-point projection of the central line of the side-look region has been developed, and the formula for the SOC has been derived. The research contributions here include the equatorial transformation, the SOC projection, the inverse transformation and a distortion analysis. As an example, image data for the SEASAT satellite has been used to establish the framework for SOC, and the coordinates of SOC has been calculated.

A new method of space map projection has been proposed. Space map projections already established are the Space Oblique Mercator, the space azimuth projection based on the tangent plane as the projection plane and the space cylinder projection based on the cylinder' surface as the projection plane. In this paper, we establish a space projection based on a cone as the projection plane, the SOC. The formula of SOC has been derived, adding a new space map projection model to the theory of space map projection.

Lastly, a more suitable dynamical mathematical foundation was established for the image data of satellite-based side-looking radar. We hope that this direct projection is of value for cartography based on remote sensing and for the precise rectification of side-looking radar imagery, both past and future.

Acknowledgement

This research was funded by the National Natural Science Foundation of China (No.41071287)

References

- Butcher, J. C. (2003) *Numerical Methods for Ordinary Differential Equations*, New York: Wiley.
- Cheng, Y. (1996) The conformal space projection. *Cartography and Geographic Information Systems*, 23, 1, 37-50.
- Colvocoresses, A. P. (1974) Space Oblique Mercator. *Photogrammetric Engineering*, 40, 8, 921-926.
- Henderson, F.M. and Lewis, A. J. (eds) (1998) *Principles and applications of imaging radar. Manual of remote sensing: 3ed, Volume 2*. Somerset, NJ: John Wiley.
- Junkins, J. L. and Turner, J. D. (1977) *Formulation of a space oblique Mercator map projection*. University of Virginia.
- Leberl, F. (1976) Imaging radar applications in mapping and charting. *Photogrammetria*. 32, 75-100.
- Leberl, F. (1981) *The radar imagery applied to mapping and charting. Translation corpus of remote sensing*. Beijing: Surveying and Mapping Press.
- Liucheng, R., Clarke, K. C. Zhou, C. et al. (2010) Geometric rectification of satellite imagery with minimal ground control using space oblique Mercator projection theory. *Cartography and Geographic Information Science*, 37, 4, 261-272.
- Ren, L.C and Zhu, C.G. (2001) SOM method of the geometric rectification for TM image processing. *Journal of Remote Sensing*, 5, 4, 295—299.
- Ren, L.C (2003) *Theory of Space Projection and its applications in Remote Sensing Technology*. Beijing: Science Press.
- Simonett, D. S. (1970) Remote Sensing with imaging radar. *Geoforum*. 2, 61-74.
- Snyder, J. P. (1977) *Space oblique Mercator projection mathematical development*. United States Geological Survey Bulletin 1518.
- Wu, Z. and Yang, Q. (1989) *Principles of mathematical cartography* (in Chinese). Beijing: Surveying and Mapping Press.
- Yang, Q. (1989) *Principles and methods of map projection transformation* (in Chinese). Beijing: PLA. Press.
- Yang, Q., Snyder, J. P., and Tobler, W. R. (1999) *Map projection transformation—Principles and Applications*, London: Taylor & Francis.
- Zhenbo Qian, et.al. (1992) *Space photographic surveying* (in Chinese). Beijing: PLA. Press.

Liucheng Ren Institute of Remote Sensing Applications, Chinese Academy of Sciences, and Air Force Command College, Beijing, China, formerly visiting scholar in the Department of Geography, University of California, Santa Barbara, CA, USA. Mail Address: #1805, No.88, Beisihuanxilu, Haidian District, Beijing, China, Zip code 100097 (renliucheng1@yahoo.com)

Keith C. Clarke Department of Geography, University of California, Santa Barbara, CA, USA, 93106-4060 (kclarke@geog.ucsb.edu)

Chenghu Zhou State Key Laboratory of Resources & Environmental Information Systems, Institute of Geography, Chinese Academy of Sciences, Beijing, China, Zip code 100101 (zhouch@lreis.ac.cn)